Evaluation of cloudiness and snowfall simulated by a semi-spectral and a bulk-parameterization scheme of cloud microphysics for the passage of a Baltic heat cyclone - First results

Armin Raabe and Nicole Mölders

Summary

The differences in the concepts of two different parameterizations of cloud microphysics are analyzed. Simulations alternatively applying these parameterizations are performed for a Baltic heat cyclone event. The results of the simulations are compared to each other as well as to observed distributions of cloudiness and snowfall. The main differences between the simulated distributions result from the assumptions on ice, the ice classes, and size distributions of the cloud and precipitating particles. Both schemes succeeded in predicting the position and the main structure of the main cloud and snowfall fields. Nevertheless, the more convective type parameterization overestimates, while the other one underestimates snowfall.

Zusammenfassung

Die Unterschiede in den Konzepten zweier unterschiedlicher Parametrisierungen der Wolkenmikrophysik werden analysiert. Die Ergebnisse der Simulationen werden miteinander und mit den beobachteten Wolken- und Schneeverteilungen für eine Baltische Wärmezyklone verglichen. Die wesentlichen Unterschiede in den berechneten Verteilungen resultieren aus den verschiedenen Annahmen über Wolkeneis, die Eisklassen und die Größenverteilungen der Wolken- und Niederschlagspartikel. Beide Schemata sagen die Position und die wesentlichen Strukturen der Wolken- und Schneeverteilungen erfolgreich vorher. Dennoch überschätzt das eher konvektive Schema den Schneefall, während das andere ihn unterschätzt.

1. Introduction

It is evident that water substances can take a wide variety of forms in clouds. These various forms develop under the influence of the seven basic microphysical processes, nucleation of particles, namely, vapor diffusion, collection, breakup of drops, fallout, ice enhancement, melting (Houze 1993). In the last decades, various cloud schemes were developed for simulating various phenomena (e.g., Cotton et al. 1982, Lin et al. 1983, McCumber et al. 1991, Flatøy 1992, Devantier and Raabe 1996, Mölders et al. 1994, 1995, 1997). Hence, in their development, special focus was on the respective phenomenon of interest. Therefore, it has to be expected that they describe the processes of the phenomenon for which they were intended with a higher accuracy than other phenomena, because the parameters are usually chosen adequate to the purposes for which the module is foreseen (Mölders et al. 1997).

In this study, two parameterizations of microphysics (Devantier and Raabe 1996, Mölders et al. 1997) applied at the Leipzig Institute for Meteorology within the framework of the non-hydrostatic meteorological model GESIMA (Kapitza and Eppel 1992, Eppel et al. 1995) are compared to each other (e.g., Fig. 1). The first module (Devantier and Raabe 1996), called DR-scheme hereafter, was developed to simulate Baltic heat cyclones (see Devantier 1995). It is a so-called semi-spectral scheme. The second module, denoted as M-scheme hereafter, was developed to simulate convective clouds of cold fronts on the meso-α-scale (e.g., Mölders 1993) and was further developed for the meso-β-scale within the framework of the local recycling of water (Mölders et al. 1997).

Simulations applying alternatively the two schemes are performed for the Baltic heat cyclone event observed from January, 11 to 12 1987. The results obtained are compared to each other and evaluated by means of observed precipitation and cloudiness (Figs. 2-7). The precipitation data of the Baltic basin were taken from the BALTEX-data bank. Those of the Elbe basin were provided by the German Weather Service.

A Baltic heat cyclones is mesoscale weather phenomenon that is built sometimes in winter when cold air flows from Scandinavia over the relative warm (some degrees °C above zero) water of the Baltic Sea (e.g., Tiesel 1984). The differences in the surface temperatures of the water and the air yield to cloud formation and heavy precipitation.

2. Analysis of microphysical parameterizations

A detailed description of GESIMA is given in Mölders (1999; this issue). Therefore, here focus is on the main parameters and parameterizations which are in common or different in the DR- and M-scheme. Figure 1 and tables 1 to 3 compare the parameterizations and the parameters used. Common to both schemes is the following:

- The fall velocities of cloud droplets are assumed to be zero.
- Following Srivastava (1967), mass-weighted mean terminal velocities are calculated for the hydrometeors.
- The same formulation of the distribution parameter is used for frozen particles.
- Both schemes use the same parameterization for the melting of ice.
- Marshall-Palmer-distributions are assumed for the spectral density of frozen particles.
- Supercooled water and ice may coexist in the temperature range between -35°C and 0°C.
- The terminal velocity of ice is determined in the same manner, except that the density correction term is optionally in the M-scheme and will not be used in the simulations presented here.
- Although freezing of rainwater is parameterized the same way in both the scheme, the resulting solid phases are different, namely *snow* in the DR-scheme and *graupel* in the M-scheme.

The main difference is that in the DR-scheme *ice* is divided into *cloud-ice* without sedimentation, *snow* and *graupel* which both sedimentate. Since only few cloud condensation nuclei act as ice nuclei (e.g., Heymsfield and Sabin 1989) and, hence, the size distributions of ice clouds are spread over few large particles, quickly developing fallspeeds of tens of cm/s (e.g., Heymsfield 1977), in the M-scheme sedimentation is immediately considered after ice has been formed. Therefore, *cloud-ice* and *snow* are not distinguished and are referred to as *ice*. Moreover, the schemes differ by the following:

- While in the M-scheme a Marshall-Palmer-distribution is assumed for the spectral density of rainwater and a mono-dispers distribution is assumed for cloud water, in the DR-scheme for liquid water log-normal-distributions are applied.
- Different parameterizations are used for condensation, evaporation, coalescence, accretion of ice by cloud water, freezing of cloud water.
- The terminal velocity of *graupel* differs by the assumed graupel-type and the formulation of the density correction term.
- In the determination of the accretion of cloud water by ice, three different ice crystal types are accounted for, while in the DR-scheme always the same ice crystal type is assumed.

The M-scheme includes the initiation of graupel for which no equivalent exists in the DR-scheme. Since in the DR-scheme, three ice classes are distinguished (Fig. 1), parameterizations to describe the interaction among these ice classes are included. Herein, the interaction between ice particles of different classes may form an ice particle of the third ice class. Hence, the following processes are considered in the DR-scheme (Note that some of them are included in 'lumped form' in the M-scheme.):

- accretion of *cloud water* and *rainwater* by *snow*,
- accretion of *graupel* by *snow*,

Tab. 1. *Comparison of the bulk-microphysics. The first subscript denotes the water phase which is reduced and the second one the water phase which is growing due to the process. Parameterizations are taken from [1] Devantier (1995), [2] Cotton et al. (1982), [3] Lin et al. (1983), [4] Cotton & Tripoli (1982), [5] Meyers et al. (1992), [6] Mölders et al. (1995), [7] Nickerson et al. (1987), [8] Kessler (1969), [9] Lui & Orville (1969), [10] Lord et al. (1984), [11] Marshall & Palmer (1948), [12] Orville & Kopp (1977), [13] Wisner et al. (1972), [14] Cotton et al. (1986), [15] Murakani (1990), [16] Locatelli & Hobbs (1974), [17] Flatøy (1992).*

	DR-Scheme	reference	M-Scheme	reference
Accretion cloud water - graupel	$CL_{cg} = \pi^2\rho_r(24\rho_a)^{-1}(\rho_o/\rho_a)^{0.5}E_{cg}N_cN_{og}a_g\Gamma(3+b_g)\ \lambda_g^{-(3+b_g)}$ $D_{co}^3\exp(9/2\ \ln^2\sigma_c)$	[1]	$CL_{cg} = 1.16(g/C_D)^{1/2}(\rho_a/\rho_g)^{1/3}(N_{og}/\lambda_g)^{1/6}E_{cg}q_cq_g^{5/6}$	[2]
Accretion cloud water - snow	$CL_{cs} = \pi^2\rho_r(24\rho_a)^{-1}(\rho_o/\rho_a)^{0.5}E_{cs}N_cN_{os}a_s\Gamma(3+b_s)\ \lambda_s^{-(3+b_s)}$ $D_{co}^3\exp(9/2\ \ln^2\sigma_c)$	[1]	-.-	-.-
Accretion rain-water - snow	$CL_{rs} = H_{rs}\ (I_{LN}^{(5)}(\sigma_r)\ I_{MP}^{(0)}(\lambda_s)+2\ I_{LN}^{(4)}(\sigma_r)\ I_{MP}^{(1)}(\lambda_s)$ $+ I_{LN}^{(3)}(\sigma_r)\ I_{MP}^{(2)}(\lambda_s))$	[1]	-.-	-.-
Accretion rain-water - graupel	$CL_{rg}^{dry} = H_{rg}\ (I_{LN}^{(5)}(\sigma_r)\ I_{MP}^{(0)}(\lambda_s)+2\ I_{LN}^{(4)}(\sigma_r)\ I_{MP}^{(1)}(\lambda_s)$ $+ I_{LN}^{(3)}(\sigma_r)\ I_{MP}^{(2)}(\lambda_s))$ $CL_{rg}^{wet} = 2\pi(\rho_rL_vD_v-K_a\Delta T)/(L_s+c_w\Delta T)N_{og}\{0.78\lambda_g^{-2}$ $+ 0.32S_c^{1/3}\Gamma[(b_g+5)/2]a_r^{1/2}\nu^{-1/2}\lambda_r^{-(b_r+5)/2}\}(\rho_o/\rho_a)^{-1}$	[1]	-.-	-.-
Accretion ice - graupel	$CL_{ig} = 0.25\ E_{ig}\pi N_{og}a_g\Gamma(3+b_g)q_i\lambda_g^{-(3+b_g)}\ (\rho_o/\rho_a)^{c_g}$	[3]	-.-	-.-
Accretion ice - ice	$CN_{is} = q_i/\delta t$	[1]	-.-	-.-
Accretion snow - graupel	$CL_{sg} = \pi^2E_{sg}N_{os}N_{og}g'(u_s,u_g)q_s\rho_s\rho_a^{-1}$ $(5/(\lambda_s^6\lambda_g) + 2/(\lambda_s^5\lambda_g^2) + 0.5/(\lambda_s^4\lambda_g^3)$	[3]	-.-	-.-
Accretion ice - cloud water	0	[4]	* $CL_{ci} = 0.25E_{ci}\pi N_iu_iq_cD_i^2$	[2], [5], [6]
Accretion ice - snow	$CL_{is} = 0.25\ E_{is}\pi N_{os}a_s\Gamma(3+b_s)q_s\lambda_s^{-(3+b_s)}\ (\rho_o/\rho_a)^{c_s}$	[3]	-.-	-.-
Accretion ice - rainwater	$CL_{ci} = q_i\pi^2(24m_i)^{-1}\rho_wE_{ir}N_ra_rD_{ro}^{5+b_r}$ $\exp(0.5(5+b_r)^2\ln^2\sigma_r)(\rho_o/\rho_a)^{1/2}$	[3]	-.-	-.-
Autoconversion cloud water to rainwater	$CN_{cr}=\max(0,\ 0.0067\rho_aq_c^2(10^{16}(\rho_aq_c/N_c)^{1.33}(\exp(9\sigma^2)-1)^{1/2}-2.7)$ $(10^4(\rho_aq_c(\exp(9\sigma^2)-1)^{0.5}/N_c)^{1/3}-1.2)$	[7]	$CN_{cr} = \max(0,\ k_1(q_c - q_{co}))$	[8]
Autoconversion cloud-ice to snow	$CN_{is} = \max(0,\ 10^{-3}\exp(0.025(T-T_o))(q_i - q_{io}))$	[3]	-.-	-.-
Coalescence	$CL_{cr} = 3\ \rho_a\ q_rq_c\ u_r\ /(2\rho_r\ (6\rho_rq_r\exp(3\ \ln^2\sigma_c)/(\pi\ \rho_rN_r))^{1/3})$	[4]	$CL_{cr} = 0.25\ E_{cr}\pi N_{or}a_r\Gamma(3+b_r)q_c\lambda_r^{-(3+b_r)}$	[9]
Condensation/ Evaporation	$CD_{vk}=0.5\rho_a^{-1}\pi S_wN_r(2G_l(T,P))^{-1}\ (0.572\ D_{ro}\exp(\ln^2\sigma_r/2)$ $+ 5310\ D_{ro}^2\exp(2\ln^2\sigma_r) - 433000\ D_{ro}^3\exp(9/2\ \ln^2\sigma_r)$	[7]	$CD_{vk} = \begin{cases} (q_v - q_{sw})r_{vc}/\delta t & \text{for } T > T_o \\ (q_v - q_s)\alpha_kr_{vk}/\delta t & \text{for } T_{oo} \le T \le T_o \text{ and } k = c,\ i \\ (q_v - q_{si})r_{vi}/\delta t & \text{for } T < T_{oo} \end{cases}$	[10]

Tab. 1 continued

distribution-parameter	$\lambda_k = (\pi\rho_k N_{ok})^{1/4}(\rho_a q_k)^{-1/4}$ für k = s, g ln-distributed for k = c, r	[11], [1]	$\lambda_k = (\pi\rho_k N_{ok})^{1/4}(\rho_a q_k)^{-1/4}$ for k = r, i, g	[11]
Evaporation of rainwater	$EV_{rv} = \partial N_r/\partial t$	[1]	$EV_{rv} = 2\pi(q_v/q_{sw}-1) N_{or}\{0.78\lambda_r^{-2}+0.32S_c^{1/3}\Gamma[(b_r+5)/2]a_r^{1/2}$ $\nu^{-1/2}\lambda_r^{-(b_r+5)/2}\}\rho_a^{-1}[L_v^2/(K_a R_v T^2) + 1/(\rho_a q_{sw} D_v)]^{-1}$	[12]
Freezing of cloud water	$FR_{ci} = q_c/\delta t$ for $T < T_{00}$ $FR_{cs} = \pi^2 B' N_c D_{co}^6 \rho_r(\rho_a 36)^{-1}\exp(A'(T_o - T)) - 1) \exp(18 \ln^2\sigma_c)$	[2], [13]	$FR_{ci} = n\, q_c/\delta t$ for $T < T_{00}$	[2]
Freezing of rainwater	$FR_{rs} = 20\pi^2 B' N_{or}\rho_r\rho_a^{-1}\exp(A'(T_o - T)) - 1)\lambda_r^{-7}$	[13]	$FR_{rg} = 20\pi^2 B' N_{or}\rho_r\rho_a^{-1}\exp(A'(T_o - T)) - 1)\lambda_r^{-7}$	[13]
Initiation of graupel	$CN_{cr} = \max(0, 10^{-3}\exp(0.09(T-T_o))(q_s - q_{so}))$	[13]	$CN_{cg} = \max(CL_{ci} - C_m N_i/\rho_a, 0)$	[2]
Melting of graupel	$ML_{gr}=-2\pi(\rho_a L_f)^{-1}[K_a(T_o-T)-\rho_a L_v D_v(q_{si}-q_v)]$ $N_{og}\{0.78\lambda_g^{-2}+0.32S_c^{1/3}\Gamma((b_g+5)/2)\, a_g^{1/2}(\rho_g/\rho_a)^{1/4}$ $\nu^{-1/2}\lambda_g^{-((b_g+5)/2)}\} - c_w\Delta T/L_s\partial q_g/\partial t$	[13]	$ML_{gr}=-2\pi(\rho_a L_f)^{-1}[K_a(T_o-T)-\rho_a L_v D_v(q_{si}-q_v)]$ $N_{og}\{0.78\lambda_g^{-2}+0.32S_c^{1/3}\Gamma((b_g+5)/2)\,[4g\rho_g/(3C_D\rho_a)]^{1/4}$ $\nu^{-1/2}\lambda_g^{-(b_g+5)/2)}\}$	[13]
Melting of ice	$ML_{ic} = q_i/\delta t$	[2]	$ML_{ir} = n\, q_i/\delta t$	[2]
Melting of snow	$ML_{gr}=-2\pi(\rho_a L_f)^{-1}[K_a(T_o-T)-\rho_a L_v D_v(q_{si}-q_v)]\, N_{os}\{0.78\lambda_s^{-2}+0.32$ $S_c^{1/3}\Gamma((b_s+5)/2)a_s^{1/2}(\rho_o/\rho_a)^{1/4}\nu^{-1/2}\lambda_s^{-(3+b_s)}\}-c_w\Delta T/L_s\partial q_s/\partial t$	[13]	-.-	-.-
Nucleation of ice	$NU_{vi} = \rho_a^{-1}4\cdot10^{-7}m_{oi}2\pi D_c N_c N_{Ao}(270.15-T)^{1/3}$	[14]	* $N_i=\max(\exp(-0.639+12.96(q_v/q_{si}-1))\rho_a q_i/2.49\bullet10^{-7})$	[6]
Sublimation of/ deposition onto graupel	$SU_{gv}=2\pi S_i\rho_a^{-1}N_{og}[0.78\lambda_g^{-2}+0.32S_c^{1/3}\Gamma((5+b_g)/2)$ $a_g^{1/2}(\rho_g/\rho_a)^{1/4}\nu^{-1/2}\lambda_g^{-((b_g+5)/2)}]$	[13]	$SU_{gv}=2\pi(q_v/q_{si}-1)/[\rho_a(L_s^2/(K_a R_v T^2) + (\rho_a q_{si} D_v)^{-1})]N_{og}$ $[0.78\lambda_g^{-2}+0.32S_c^{1/3}\Gamma((b_g+5)/2)$ $\{4g\rho_g/(3C_D\rho_a)\}^{1/4}\nu^{-1/2}\lambda_g^{-(b_g+5)/2)}]$	[13]
Sublimation of/ deposition onto snow	$SU_{sv}=2\pi S_i\rho_a^{-1}N_{os}[0.78\lambda_s^{-2}+0.32S_c^{1/3}\Gamma((5+b_s)/2)$ $a_s^{1/2}(\rho_g/\rho_a)^{1/4}\nu^{-1/2}\lambda_s^{-(b_s+5)/2)}]$	[13]	-.-	-.-
Terminal velocity of ice	$v_{Ti} = a_i\Gamma(4 + b_i)\,(6\lambda_i^{b_i})^{-1}(\rho_o/\rho_a)^{c_i}$	[15]	$v_{Ti} = a_i\Gamma(4 + b_i)(6\lambda_i^{b_i})^{-1}(\rho_o/\rho_a)^{c_i}$	[16]
Terminal velocity of graupel	$v_{Tg}= a_g\Gamma(4 + b_g)(6\lambda_g^{b_g})^{-1}(\rho_g/\rho_a)^{1/2}$	[15]	$v_{Tg} = (4g/(C_D 3))^{1/2}\Gamma(4 + b_g)(6\lambda_g^{b_g})^{-1}(\rho_g/\rho_a)^{1/2}$	[3]
Terminal velocity of rainwater	$v_{Tr} = a_r D_{or}^{b_r}\exp(\ln^2\sigma_r\,(b_r^2)/2)\,(\rho_o/\rho_a)^{c_r}$	[11], [17]	$v_{Tr} = a_r\Gamma(4 + b_r)(6\lambda_r^{b_r})^{-1}(\rho_o/\rho_a)^{c_r}$	[3]

Furthermore $H_{rs} = \pi^2\rho_r(24\rho_a)^{-1}N_r N_{os} g'(u_r,u_s)$

$H_{rg} = \pi^2\rho_r(24\rho_a)^{-1}N_r N_{og} g'(u_r,u_g)$

$E_{is} = \exp(0.025(T-T_o))$

$g'(ux,uy)=((\alpha u_x-\beta u_y)^2+\gamma u_x u_y))^{1/2}$

- melting of *snow*,
- autoconversion of *ice* to *snow*.

Tab. 2. *Diameter, D_i, terminal velocity, u_i and mass, m_i ($= \rho_a q_i / N_i$) as used in the accretion of cloud water and ice in the M-scheme.*

Ice crystal type	D_i m	u_i m/s	m_i kg	Reference
Hexagonal plates	$16.3 m_i^{1/2}$	$304 D_i (\rho_o/\rho_a)^{c_i}$	$m_i < 1.7 \cdot 10^{-10}$	Hobbs et al. (1972)
Slightly rimed plates of hexagonal type	$6.07 m_i^{1/2}$	$1250 D_i (\rho_o/\rho_a)^{c_i}$	$1.7 \cdot 10^{-10} \leq m_i < 10^{-8}$	Hobbs et al. (1972)
Graupel-like snow of hexagonal type	$1.58 m_i^{0.417}$	$4.84 D_i^{1/4} (\rho_o/\rho_a)^{c_i}$	$10^{-8} \leq m_i < 2.49 \cdot 10^{-7}$	Locatelli & Hobbs (1974)

Tab. 3. *Parameters as used in the parameterizations.*

	DR-Scheme		M-Scheme	
a_g	$124\ m^{0.36}\ s^{-1}$	Devantier (1995)	$1\ m^{0.5}\ s^{-1}$	Lin et al. (1983)
a_i	$700\ s^{-1}$	Murakami (1990)	$56.4\ m^{0.43}\ s^{-1}$	Locatelli & Hobbs (1974)
a_r	$842\ m^{0.2}\ s^{-1}$	Lui & Orville (1969)	same	same
a_s	$17\ m^{0.5}\ s^{-1}$	Murakami (1990)	-.-	-.-
b_g	0.64	Devantier (1995)	0.5	Lin et al. (1983)
b_i	1	Murakami (1990)	0.57	Locatelli & Hobbs (1974)
b_r	0.8	Lui & Orville (1969)	same	same
b_s	0.5	Murakami (1990)	-.-	-.-
c_g	0.5	Devantier & Raabe (1996)	-.-	-.-
c_i	0.35	Devantier & Raabe (1996)	0.5	Cotton et al. (1982)
c_r	0.5	Cotton et al. (1982)	same	same
c_s	0.5	Cotton et al. (1982)	same	same
k_1	-.-	-.-	$10^{-3}\ s^{-1}$	Kessler (1969)
q_{co}	-.-	-.-	$5 \cdot 10^{-4}$ kg/kg	Kessler (1969)
q_{so}	$6 \cdot 10^{-4}$ kg/kg	Lin et al. (1983)	-.-	-.-
A'	$0.66\ K^{-1}$	Bigg (1953)	same	same
B'	$100\ m^{-3}\ s^{-1}$	Bigg (1953)	same	same
C_D	-.-	-.-	0.6	Wisner et al. (1972)
C_m	-.-	-.-	$10^{-9}\ kg\ s^{-1}$	Cotton et al. (1982)
D_{oc}^{ini}	$10 \cdot 10^{-6}$ m	Devantier (1995)	-.-	-.-
D_{or}^{ini}	$32.5 \cdot 10^{-6}$ m	Devantier (1995)	-.-	-.-
E_{cg}	-.-	-.-	0.5	Mölders et al. (1997)
E_{ci}	0	Devantier (1995)	0.8	Heymsfield & Sabin (1989)
E_{cr}	0.1	Devantier (1995)	1	Lin et al. (1983)
E_{ri}	1	Devantier (1995)	-.-	-.-
E_{cs}	1	Devantier (1995)	-.-	-.-
E_{cg}	1	Devantier (1995)	-.-	-.-
E_{cc}	0.1	Devantier (1995)	-.-	-.-
E_{ig}	0.1	Devantier (1995)	-.-	-.-
E_{cg}	1	Devantier (1995)	-.-	-.-
E_{rg}	1	Devantier (1995)	-.-	-.-
N_{Ao}	$2 \cdot 10^{5}\ m^{-3}$	Devantier (1995)	-.-	-.-
N_{og}	-.-	-.-	$4 \cdot 10^{4}\ m^{-4}$	Federer & Waldvogel (1975)
N_{og}^{ini}	$1.1 \cdot 10^{6}\ m^{-4}$	Cotton & Anthes (1989)	-.-	-.-
N_{oi}	$3 \cdot 10^{6}\ m^{-4}$	Gunn & Marshall (1958)	$7.6 \cdot 10^{6}\ m^{-4}$	Leary & Houze (1979)
N_{or}	q_r/λ_r	Cotton & Anthes (1989)	$8 \cdot 10^{6}\ m^{-4}$	Marshall & Palmer (1948)
N_{os}^{ini}	$32.5 \cdot 10^{6}\ m^{-4}$	Cotton & Anthes (1989)	-.-	-.-
λ_g^{ini}	0.6	Cotton & Anthes (1989)	-.-	-.-
λ_s^{ini}	0.25	Cotton & Anthes (1989)	-.-	-.-

Tab. 3 *continued*

ρ_r	1000 kg m^{-3}	-.-	same	-.-
ρ_i	500 kg m^{-3}	Devantier (1995)	84 kg m^{-3}	Heymsfield & Sabin (1989)
ρ_s	84 kg m^{-3}	Heymsfield & Sabin (1989)	-.-	-.-
ρ_g	200 kg m^{-3}	Devantier (1995)	600 kg m^{-3}	Cotton et al. (1982)
$\ln \sigma_i$	0.25	Nickerson et al. (1987)	-.-	-.-
$\ln \sigma_c$	0.28	Nickerson et al. (1987)	-.-	-.-
$\ln \sigma_r$	0.5	Nickerson et al. (1987)	-.-	-.-

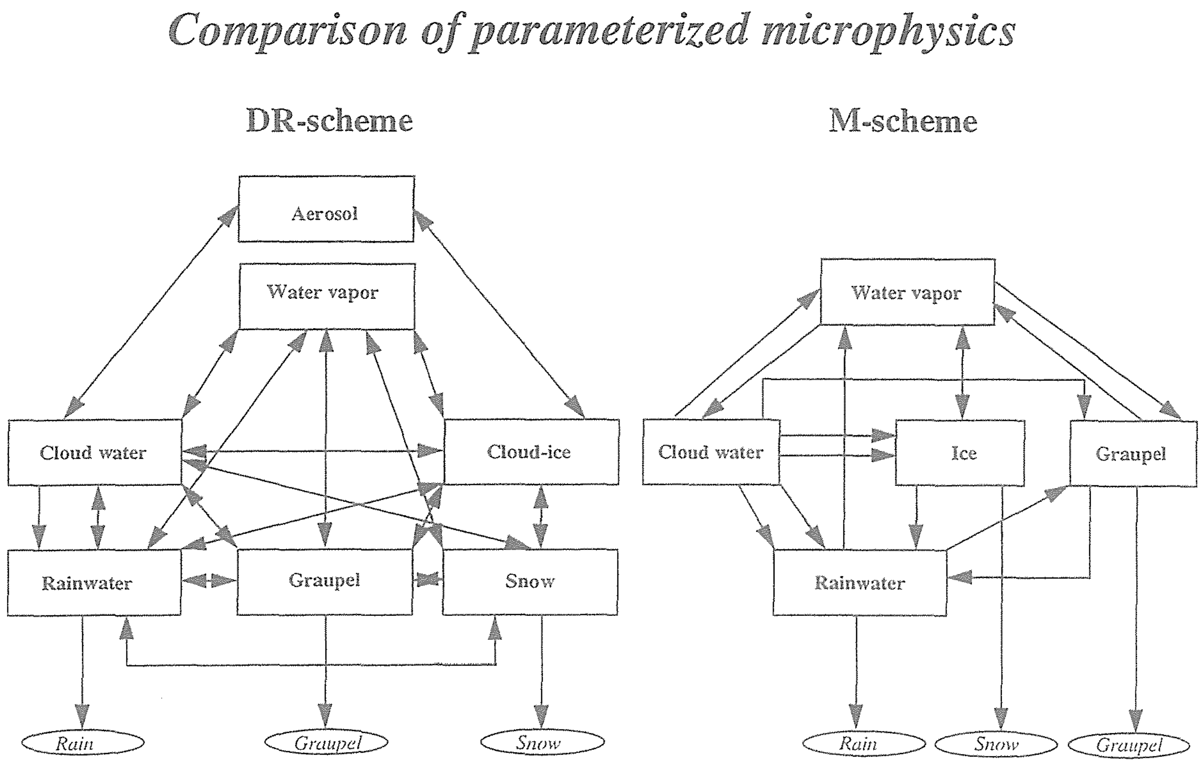

Fig. 1. Schematic view of the microphysical processes considered in the DR-scheme and the M-scheme, respectively.

3. Comparison of the simulation results

In both the simulations the near surface wind field converges over the Mecklenburger Bucht and the Pommersche Bucht. This moisture convergence leads to upward motions and cloud formation. Comparing the simulated cloud distributions shows that the cloud fields provided by the DR-scheme cover a larger area than those provided by the M-scheme (Figs. 3, 4). The same is true for the extension of the snow fields (Figs. 6, 7). These larger extensions may be explained by the postulation of non-sedimentating *cloud-ice*. Non-sedimentating *cloud-ice* rests at a cloud level until it either sublimates or until it converts to *snow*. Hence, in the DR-scheme, *cloud-ice* spreads more widely by diffusion and advection than *ice* in the M-scheme. The concept of non-sedimentating *cloud-ice* also retards the formation of precipitating particles and may contribute to the lower snowfall rates of the DR-scheme as compared to the M-scheme.

The results of a sensitivity study, for which in the M-scheme *ice* had to exceed a critical mass of $5 \cdot 10^{-9}$ kg before sedimentation starts, the distributions of cloudiness slightly differed from those of the origin formulation (Mölders 1993). Similar was also found by Cho

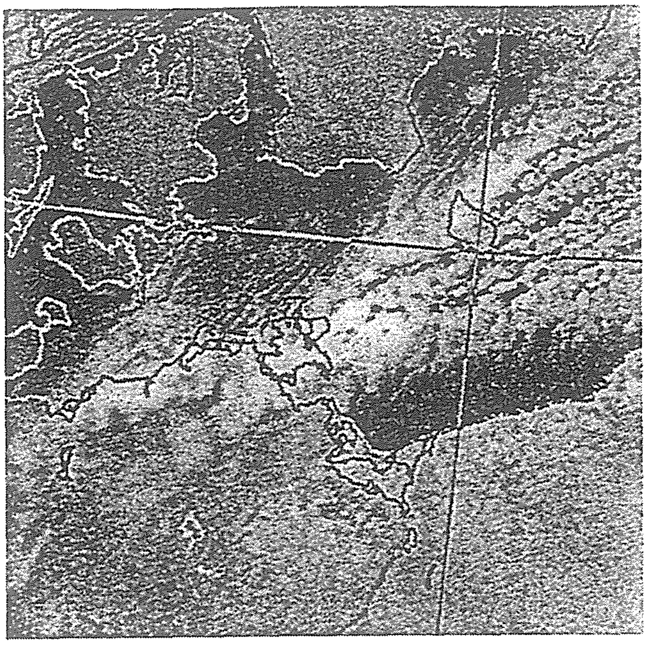

Fig. 2. NOAA-9 AVHRR IR-imagery of cloud distribution at 11 January 1987 1236 UTC (from Pike 1990).

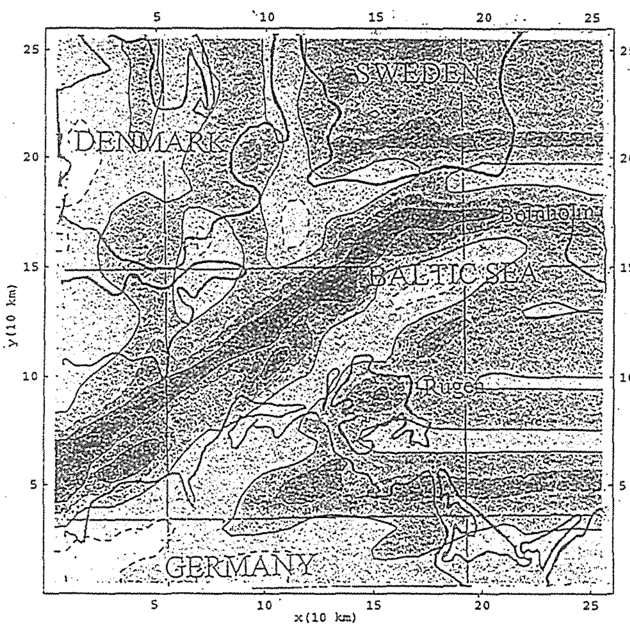

Fig. 3. Mean distribution of cloud water as obtainted from the simulation with the DR-scheme. The grey labels reach from 0.01 g/kg in white to 0.1 g/kg in black.

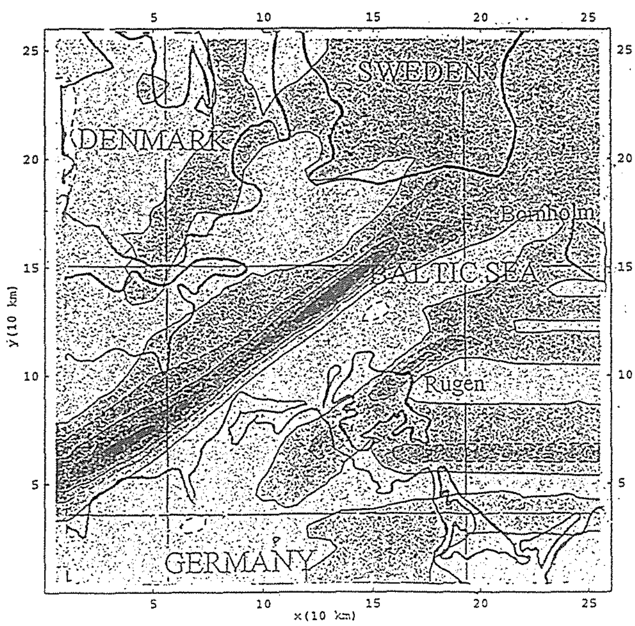

Fig. 4. Like Fig. 3, but for the simulation with the M-scheme.

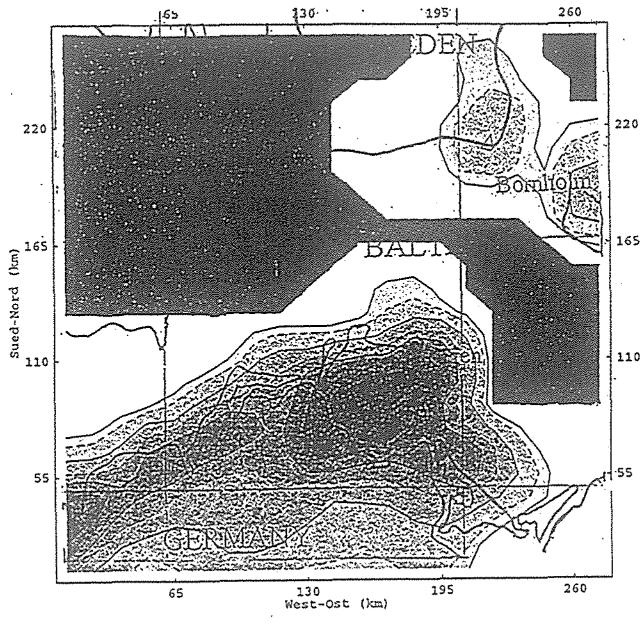

Fig. 5. Observed precipitation over the south-western Baltic Sea on January, 11 1987. White areas indicate no snowfall observed. Black areas indicate areas without observatinal data. Grey levels (from light to dark) are at 0.5, 1, 2.5, 5, 7.5, 10, 15, 20, 25 mm.

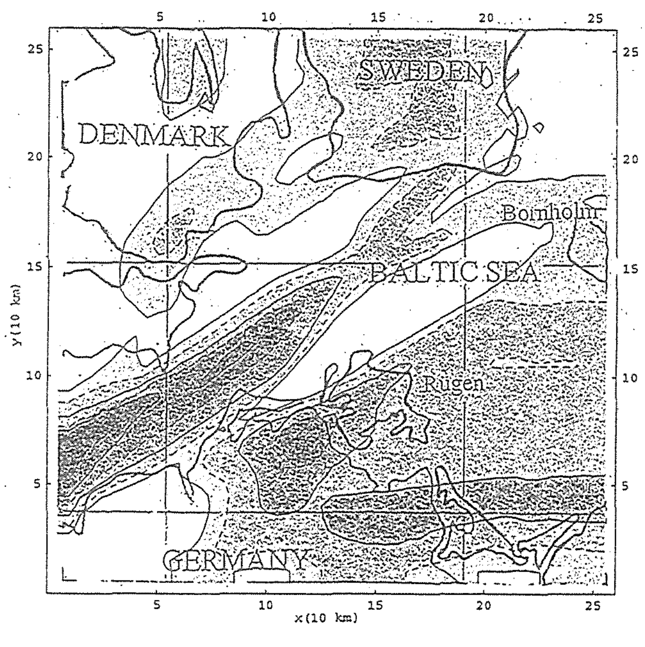

Fig. 6. Precipitation as simulated by the DR-scheme.Grey levels (from light to dark) are at 0.5, 1, 2.5, 5, 7.5, 10, 15, 20, 25 mm.

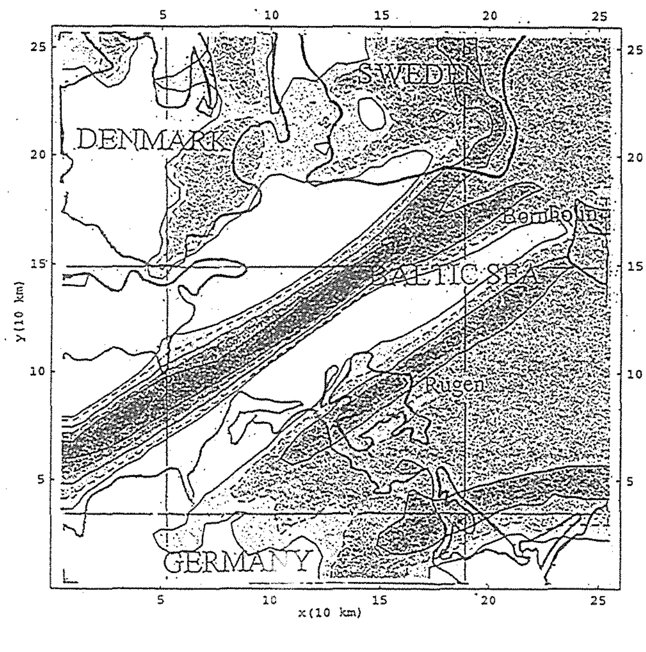

Fig. 7. Precipitation as simulated by the M-scheme. Grey levels (from light to dark) are at 0.5, 1, 2.5, 5, 7.5, 10, 15, 20, 25 mm.

et al. (1989). In the evaluation of precipitation, however, BIAS and threat-score became slightly worse as compared to those obtained from the version with immediate onset of sedimentation (Mölders 1993).

Further differences may result from the use or neglecting of the density correction term. Sensitivity studies performed with the M-scheme with and without a density correction term showed the following (Mölders 1993). The cloud tops are found in lower levels because of the increase in the fall velocity of the particles in upper levels. Hence, the enhanced removal of condensate from the upper levels reduces relative humidity. Since cloud water does not sedimentate, more cloud water exists in the upper levels in the study with density correction than in that without. The altered terminal velocity indirectly affect cloud water via the changed distributions of rainwater and ice and accretion rates. On average, the inclusion of the correction term reduces the mixing ratios of rainwater and ice. This is due to the fact that in the upper part of the clouds less time is available for accretion, and in the lower part of the atmosphere more time is available for sublimation and evaporation. The accumulated precipitation may both decrease or increase. Mölders (1993) found for a 3 day period in springtime that the inclusion of the correction term may lead to an increase of the 72h-accumulated precipitation by more than 7.5 mm at one location, while it yields in a decrease by 3.1 mm at another.

4. Comparison simulated cloudiness and snowfall to observations

The simulations were performed assuming a constant geostrophic wind speed and direction in the upper levels. Since in nature, however, the speed and the direction of the flow slightly vary with time, it is obvious that the simulation results differ to a certain degree from the observation. Comparing the simulated (Figs. 3, 4) and the observed cloud distributions (Fig. 2) shows satisfactory results for both the simulations. The satellite data show thin cirrus over large areas of the Baltic. In the upper levels, both schemes also provide slight ice amounts over nearly the entire domain. Both schemes predict the main cloud bands at nearly the right positions except for the cloud band over Denmark (see upper edge of the model domain). These clouds are not predicted by both the simulations. Here, the formulation of the boundaries are the reason. While the simulation applying the DR-scheme better provides the heterogeneous structure of the cloud band in the south-western part of the Mecklenburger Bucht, the simulation using the M-scheme better succeeds in predicting the double-band structure in the north-eastern part of that cloud band.

Comparing the simulated (Figs. 6, 7) and the observed precipitation distribution (Fig. 5) shows that both schemes satisfyingly predict the position of the snow field. Taking into account that no data were reported over the Baltic Sea, and that clouds of similar appearence than the snow providing clouds over land were observed by satellite, it has to be expected that the line-like form of the snow field, which is predicted by the two simulations, may be reliable. Moreover, the reanalysis of this event also provides a snow band over the Baltic Sea (e.g., Gustafsson et al. 1998) as do our simulations. Comparing only the simulated and observed snow fields on land differences can be found in the position of the snowfall maxima as well as in the extension of the snow field. While the DR-scheme under-estimates maximum snowfall, the M-scheme over-estimates the maximum values. The discrepancies with respect to the maxima may be due to differences between the ice crystal types, ice density and, hence, the deviating terminal velocities of the frozen particles in nature and the model world.

5. Conclusions

Two different parameterization schemes of cloud microphysics were compared to each other and observed snowfall to elucidate their impact on predicted snowfall. The important processes used in both the parameterization schemes are nucleation, vapor diffusion, collection, and melting, as well as fallout. While one of the schemes subdivides the frozen particles into (sedimentating) *ice* and *graupel*, the other one distinguishes between (non-sedimentating) *cloud-ice*, *snow*, and *graupel*. The impact of *graupel* and *rainwater* was small in our case study. The main differences between the parameterization schemes are the assumptions made on the heterogeneous ice forming processes, on the form and density of the ice as well as on the size distributions of the water substances.

The evaluation showed that both the cloud modules are able to realistically simulate the cloud and snowfall distributions associated with the Baltic heat cyclone of 11/12 January 1987. The discrepancies between the simulated and observed maxima may be due to the assumptions on the ice characteristics and classes, which among others restrict the amount of different ice cyrstal types occurring. The settling of the frozen particles strongly depends on the ice crystal type. Hence, the evaluation suggests that more ice crystal types should be considered in the parameterizations so that the cloud formation may better adjust to the synoptic situation to be simulated.

Up to now only a visual evaluation was carried out which may not allow to point out which scheme predicted the examined Baltic heat cyclone event the most appropriate. Therefore, an objective evaluation by use of scores (threat scores, BIAS-score, probability of detection, categorical score, rms-score, etc.) as performed by Mölders (1993) is planned for the future.

Acknowledgements

We would like to express our thanks to the Ministry of Education, Science and Technology (BMBF) and the Deutsche Forschungsgemeinschaft (DFG) for the support of this study under contracts 07KTF83, 01LA9839/4, Mo770/1-1 and Mo770/1-2. We also thank M. Klingspohn for helpful comments. The precipitation data were provided by the BALTEX-data bank as well as by the German Weather Service.

References

Bigg, E.K. 1953. The supercooling of water. Proc. Phys. Soc., London B66, 668-694.

Cho, H.R., M. Niewiadomski, J.V. Iribarne, O. Melo, 1989. A model of the effect of cumulus clouds on the redistribution and transformation of pollutants. *J. Geophys. Res.* 94: 12895-12910.

Cotton, W.R., R.A. Anthes, 1989. *Storms and cloud dynamics*. Academic Press, San Diego.

Cotton, W.R., M.A. Stephens, T. Nehrkorn, G.J. Tripoli, 1982. The Colorado State University three-dimensional cloud/mesoscale model. Part II: An ice phase parameterization. *J. Rech. Atmos.* 16: 295-320.

Cotton, W.R., G.J.Tripoli, R.M.Rauber, E.A.Mulivihill, 1986. Numerical simulations of the effects of varying ice crystal nucleation rates and aggreation processes on orographic snowfall. *J. Clim. Appl. Meteor.* 25: 1658-1680.

Devantier, R., 1995. Wolkenbildungsprozesse über der südlichen Ostsee - Anwendungen eines neuen Wolkenschemas in einem mesoskaligen Modell. Ph.D. thesis, Univ. Leipzig.

Devantier, R., A. Raabe, 1996. Application of a quasispectral cloud parameterization scheme to a mesoscale snowfall event over the Baltic Sea. *Contrib. Atmos. Phys.* 69: 375-384.

Eppel, D.P., H. Kapitza, M. Claussen, D. Jacob, W. Koch, L. Levkov, H.-T. Mengelkamp, N. Werrmann, 1995. The non-hydrostatic mesoscale model GESIMA. Part II: Parameterizations and applications. *Contrib. Atmos. Phys.* 68: 15-41.

Federer, B., A. Waldvogel, 1975. Hail and raindrop size distributions from a Swiss multicell storm. *J. Appl. Meteor.* 14, 91-97.

Flatøy, F. 1992. Comparison of two parameterization schemes for cloud and precipitation processes. *Tellus* 44A: 41-53.

Gunn, K.L.S., J.S. Marshall, 1958. The distribution with size of aggregate snowflakes. *J. Meteor.* 15: 452-461.

Gustafsson, N., A. Omstedt, L. Nyberg, 1998. Coupling high resolution atmosphere and ocean models for the Baltic Sea. *Mon. Wea. Rev.* (in press).

Heymsfield, A., 1977. Precipitation development in stratiform ice clouds: A microphysical and dynamical study. *J. Atmos. Sci.* 34: 367-381.

Heymsfield, A.J., R.M. Sabin, 1989. Cirrus crystal nucleation by homogeneous freezing of solution droplets. *J. Atmos. Sci.* 46: 2252-2264.

Hobbs, P.V., L.F. Radke, A.B. Fraser, J.D. Locatelli, D.G. Robertson, R. Atkinson, J. Farber, R.R. Weiss, R.C. Easter, 1972. Field observations and theoretical studies of clouds and precipitation over the Cascade Mountains and their modification by artificial seeding (1971-1972). Res. Rep. VII, Dept. Atmos. Sci. Univ. of Wash., Seattle, 293 pp.

Houze, R.A., Jr., 1993. *Cloud Dynamics*. Academic Press, San Diego, p. 573.

Kapitza, H., D.P. Eppel, 1992. The non-hydrostatic mesoscale model GESIMA. Part I: Dynamical equations and tests. *Contrib. Atmos. Phys.* 65: 129-146.

Kessler, E., 1969. On the distribution and continuity of water substance in atmospheric circulations. *Meteor. Monogr.* 27, Amer. Meteor. Soc., 84.

Leary, C.A., R.A. Jr. Houze, 1979. Melting and evaporation of hydrometeors in precipitation from the anvil clouds of deep tropical convection. *J. Atmos. Sci.* 36: 669-679.

Lin, Y.-L., R.D. Farley, H.D. Orville, 1983. Bulk parameterization of the snow field in a cloud model. *J. Clim. Appl. Meteor.* 22: 1065-1092.

Locatelli, J.D., P. Hobbs, 1974. Fall speeds and masses of solid precipitation particles. *J. Geophys. Res.* 79: 2185-2197.

Lord, S.J., H.E. Willoughby, J.M. Piotrowicz, 1984. Role of a parameterized ice-phase microphysics in an axissymetric, nonhydrostatic tropical cyclone model. *J. Atmos. Sci.* 41: 2836-2848.

Lui, J.Y., H.D. Orville, 1969. Numerical modeling of precipitation and cloud shadow effects on mountain-induced cumuli. *J. Atmos. Sci.* 26: 1283-1298.

Marshall, J.S., W.M. Palmer, 1948. The distribution of raindrops with size. *J.Met.* 5: 165-166.

McCumber, M., W.-K. Tao, J. Simpson, R. Penc, S.-T. Soong, 1991. Comparison of ice-phase microphysical parameterization schemes using numerical simulations of tropical convection. *J. Appl. Meteor.* 30: 985-1004.

Meyers, M.P., P.J. DeMott, W.R. Cotton, 1992. New primary ice-nucleation parameterizations in an explicit cloud model. *J. Appl. Meteor.* 31: 708-721.

Mölders, N. 1993. Wolkenparametrisierung für ein Chemie-Transportmodell. *Mitt. Inst. f. Geophys. u. Meteor.* Univ. zu Köln 88, Ph. D. thesis.

Mölders, N., H. Hass, H.J. Jakobs, M. Laube, A. Ebel, 1994. Some effects of different cloud parameterizations in a mesoscale model and a chemistry transport model. *J. Appl. Meteor.* 33: 527-545.

Mölders, N., Laube, M., Kramm, G., 1995. On the parameterization of ice microphysics in a mesoscale a weather forecast model. *Atmos. Res.* 38: 207-235.

Mölders, N., Kramm, G., Laube, M., Raabe, A., 1997. On the influence of bulk parameterization schemes of cloud relevant microphysics on the predicted water cycle relevant quantities - a case study. *Meteorol. Zeitschr.* 6: 21-32.

Mölders, N., 1999. On the enhancement or counteraction of the responses to local-scale accumulated land-use changes on the short time-scale. This issue

Murakami, M., 1990. Numerical modeling of dynamical and microphysical evolution of an isolated convective cloud. *J. Met. Soc. Japan* 68: 107-127.

Nickerson, E.C., E. Richard, R. Rosset, D.R. Smith, 1987. The numerical simulation of clouds, rain and airflow over the Vosges and Black Forest Mountains: A meso-β model with parameterized microphysics. *Mon. Wea. Rev.* 114: 398-414.

Orville, H.D., F.J. Kopp, 1977. Numerical simulation of the life history of a hailstorm. *J. Atmos. Sci.* 34: 1596-1618.

Pike, W.S., 1990. A heavy mesoscale snowfall event in northern Germany. *Meteorological Magazine* 119: 187-195.

Schlamp, R.J., H.R. Pruppacher, A.E. Hamielec, 1975. A numerical investigation of the efficiency with which simple columnar ice crystals collide with supercooled water drops. *J. Atmos. Sci.* 32: 2330-2337.

Srivastava, R.C. 1967. A study of effects of precipitation on cumulus dynamics. *J. Atmos. Sci.* 24: 36-45.

Tiesel, R., 1984. Die Wärmezyklonen der westlichen und mittleren Ostsee. *Z. Meteor.* 34: 354-365.

Tripoli, G.J., W.R. Cotton, 1982. The Colorado State University Three-dimensional Cloud/ Mesoscale Model - Part I: General theoretical framework and sensitivity experiments. *J. Rech. Atmos.* 16: 185-219.

Wisner, C., H.D. Orville, C. Myers, 1972. A numerical model of a hail-bearing cloud. *J. Atmos. Sci.* 29: 1160-1181.

Addresses of the authors:
LIM - Institut für Meteorologie, Universität Leipzig, Stephanstraße 3, 04103 Leipzig